

Experimental Study of Potential Profile Formation in Large Helical Device

A. Shimizu 1), T. Ido 1), M. Nishiura 1), S. Nakamura 2), M. Nakamura 2), H. Nakano 1), M. Yokoyama 1), N. Tamura 1), H. Takahashi 1), Y. Yoshimura 1), S. Kubo 1), T. Shimozuma 1), H. Igami 1), K. Ida 1), M. Yoshinuma 1), K. Nagaoka 1), I. Yamada 1), K. Narihara 1), K. Tanaka 1), K. Kawahata 1), S. Kato 1) and LHD Group

1) National Institute for Fusion Science, 322-6 Oroshi-cho, Toki, Gifu 509-5292, Japan

2) Graduated School of Engineering, Nagoya University, Furo-cho, Nagoya 464-8601, Japan

E-mail: akihiro@nifs.ac.jp

Abstract: The radial profile of potential, ϕ , in the core region of the Large Helical Device (LHD) was measured with a Heavy Ion Beam Probe (HIBP) in wide parameter area, in which radial electric field, E_r , could not be measured in previous experiments. The radial profiles of E_r were estimated from the differentiation of the experimental data of HIBP. These E_r profiles were compared with the calculation result from neoclassical theory, and the theoretical prediction almost coincided with the experimental data of E_r in the core region of LHD plasmas.

1. Introduction

In toroidal magnetized plasmas, the radial electric field E_r is a very important parameter in transport phenomena. In the low collisional regime of helical devices, ripple induced diffusion loss is predicted from the neoclassical theory. This ripple-induced diffusion loss is non-ambipolar, so the radial electric field is formed. Diffusion loss in low collisional regime can be suppressed by the radial electric field, E_r , which is determined by the ambipolar condition. In previous experiments in LHD, charge exchange recombination spectroscopy (CXRS) was used to study E_r formation. However, most of data were obtained in the outer region ($\rho > 0.6$) of plasmas, in which helical ripple is large, because of insufficient emission from the impurities in the core region. In order to clarify physics of E_r formation in the core region, where helical ripple is relatively small, the radial profile of plasma potential was measured with Heavy Ion Beam Probe (HIBP) [1-7]. In addition, we investigated

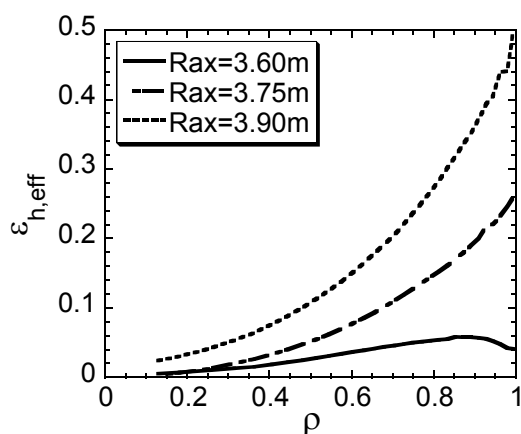


FIG.1 Radial profiles of effective helical ripple of LHD are shown.

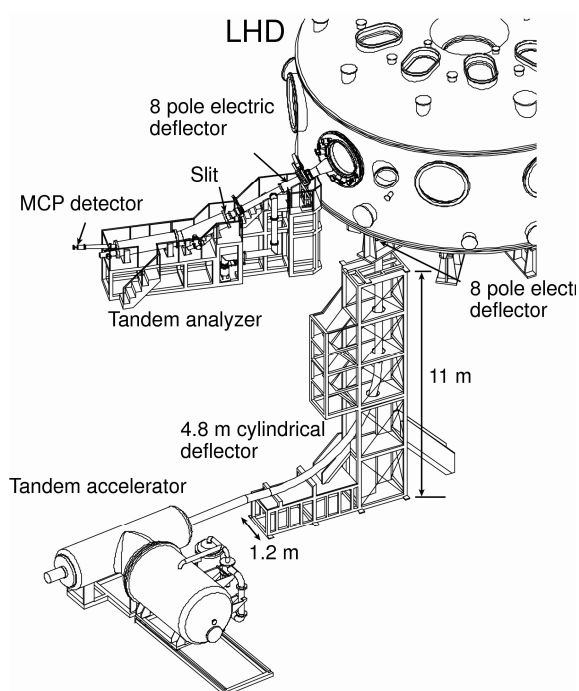


FIG. 2 Schematic view of HIBP system on LHD

E_r in wider plasma-parameter space including high ion temperature (T_i) plasmas and high electron temperature (T_e) plasmas heated by ECH (no NBI), in which the electric field measurements by CXRS is difficult.

2. Experimental setup

The Large Helical Device (LHD) is a helical device, magnetic field configuration of which is characterized by the major radius of magnetic axis, R_{ax} , the pitch parameter γ , the quadrupole field component B_q . In this article, γ and B_q are fixed as the standard one, namely $\gamma = 1.254$, $B_q = 100\%$. By changing the major radius of R_{ax} , the amount of helical ripple is changed. In the inward shifted configuration of $R_{ax} = 3.6$ m, the helical ripple is smaller than that of the outward shifted configuration, $R_{ax} = 3.9$ m. Radial profiles of effective helical ripple are shown in Fig. 1.

HIBP [1] system was installed to LHD and has been developed in many years [2-9]. A schematic view of HIBP system in LHD is shown in Fig. 2. By using the tandem accelerator, the gold ion beam (A_u^{+}), maximum energy of which is 6 MeV, is generated and it is injected to plasma as primary beam. The secondary beam (A_u^{2+}) is formed by the collision with plasma, energy of which is analyzed by the tandem energy analyzer [10]. The three dimensional orbit of probe beam is controlled by two 8-pole electrostatic deflectors [11]. The primary and secondary beam current intensity is about a few μ A and a few nA respectively. In order to detect this level of current, the sensitive current detector, micro channel plate (MCP), is used. The spatial resolution (the scale of sample volume) is about a few cm [4].

3. Experimental result

A typical shot is shown in Fig.3, when the radial profile of plasma potential was measured. The magnetic field strength, B_t was 1.5 T, and the major radius of magnetic axis, R_{ax} was 3.75 m. The plasma was produced by electron cyclotron heating (ECH) and sustained by neutral beam injection heating (NBI). Both of NBI#1 and NBI#3 are counter-direction. The toroidal current induced by these counter-direction NBIs is about 40 kA. The line averaged density gradually increased from $0.2 \times 10^{19} \text{ m}^{-3}$ to $0.5 \times 10^{19} \text{ m}^{-3}$ by gas puff control. The central electron temperature was about 2.5 keV at the line averaged density of $0.19 \times 10^{19} \text{ m}^{-3}$ and ~ 1.0 keV at the line averaged density $> 0.30 \times 10^{19} \text{ m}^{-3}$. In each period marked by alphabets A~E, the potential profile was measured with HIBP as shown in Fig.4. In the ECH phase (the duration A), the plasma potential at the center was positive. As the density increased, the potential decreased in the core region. In low density and high electron temperature case, the potential at the center tends to be positive. In high density and low electron temperature case, the potential at the center tends to be negative or nearly zero.

By using a polynomial function of ρ as a fitting function, radial electric field profile was

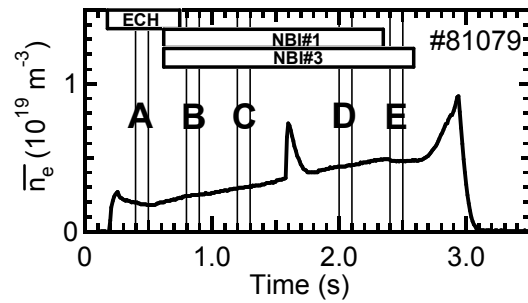


FIG.3 Typical shot when the potential profile measured with HIBP. In the duration marked by alphabets A~E, the potential profile was measured.

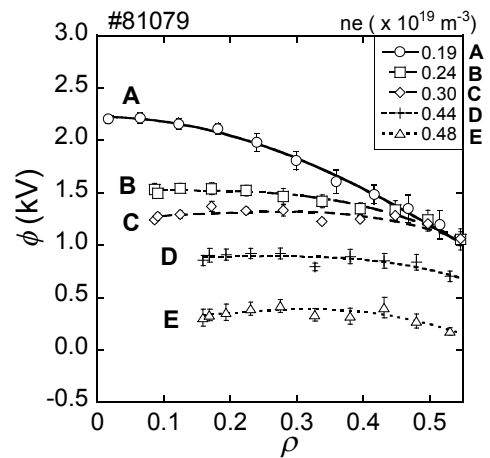


FIG.4 Potential profiles measured with HIBP is shown. Alphabets A~E correspond to time duration displayed in FIG. 2.

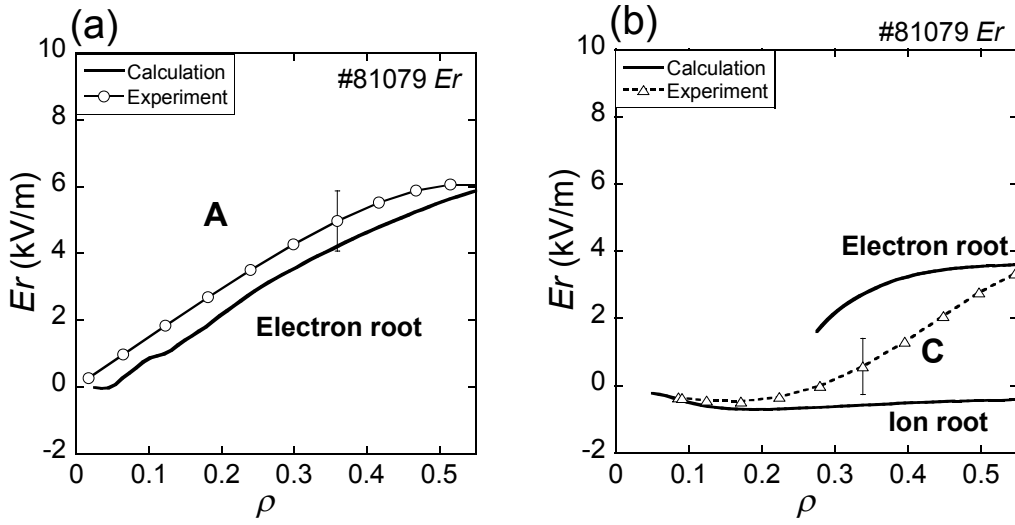


FIG.5 (a) The radial electric field profile in case A ($\bar{n}_e = 0.19 \times 10^{19} \text{ m}^{-3}$). (b) E_r in case C ($\bar{n}_e = 0.30 \times 10^{19} \text{ m}^{-3}$) in FIG.2. Open circle and diamond symbols are obtained from experimental data, and solid and dotted lines are theoretical predictions. Theoretical prediction roughly coincides with Experimental data.

obtained from the experimental data. Obtained radial electric field profiles are compared with those estimated by GSRACE code [12]. In Fig.5 (a) and (b), the comparison in period A and C are shown respectively. In the period A ($\bar{n}_e = 0.19 \times 10^{19} \text{ m}^{-3}$), from the theory the positive radial electric field, so called electron root, is predicted. And this prediction roughly coincides with the experimental results. In the period C ($\bar{n}_e = 0.30 \times 10^{19} \text{ m}^{-3}$), the negative radial electric field, so called ion root, in the core region is predicted. And in this case, in the region $\rho > 0.26$, both roots of electron and ion roots are expected. In the core region, the ion root calculated by the neoclassical theory coincides with the experimental result. In the outer region where $\rho \sim 0.6$, the electron root of theoretical prediction coincides with the experimental result.

The dependence of the sign of measured radial electric field, E_r , on the electron and ion temperatures is studied and is compared with the neoclassical prediction as shown in Fig. 6. Figure shows plasma parameters in the T_i - T_e space, and different symbol is used for each sign of E_r at the radial position of $\rho = 0.25$. The solid curves show predicted boundaries among "Electron root" (positive E_r), "Ion Root" (negative E_r) and "Multiple Root", where parabolic

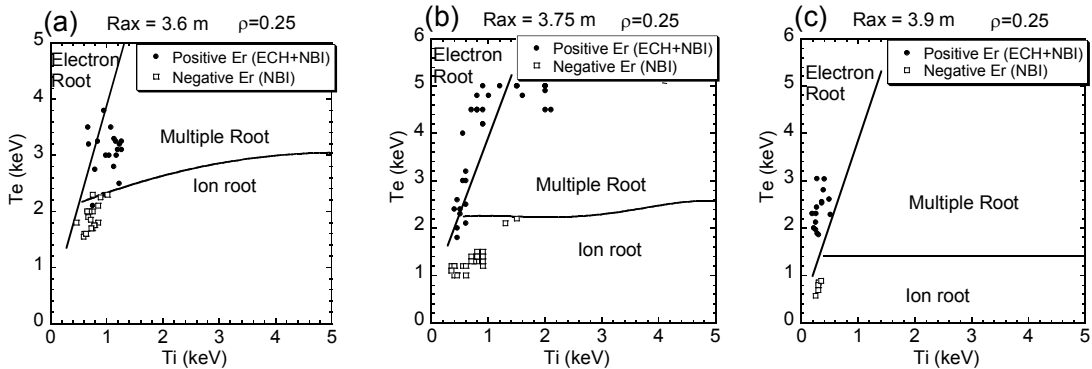


FIG.6 The parameters of electron and ion temperature, when positive E_r or negative (almost zero) E_r was observed, are shown. Solid line is the theoretical boundary, which divides T_i - T_e space into the regions where the electron root ($E_r > 0$), multiple root (both), and ion root ($E_r < 0$) are expected. (a) Inward shifted configuration, $R_{ax} = 3.6 \text{ m}$ (b) $R_{ax} = 3.75 \text{ m}$ (c) Outward shifted configuration, $R_{ax} = 3.9 \text{ m}$.

temperature profiles and the low density ($\bar{n}_e \sim 0.3 - 0.5 \times 10^{19} \text{ m}^{-3}$) are assumed [13]. The major radius of magnetic axis, R_{ax} , of magnetic configuration is 3.6 m for Fig. 6(a), 3.75 m for Fig. 6(b), and 3.9 m for Fig. 6(c). In the case of high T_e plasma with the electron internal transport barrier (e-ITB) [16-17], a positive radial electric field was observed. These shots are in "Electron Root" or "Multiple Root" regime in Fig.6. The experimental parameters of the case A in Fig.4 are in this regime. If the parameters are in the "Ion root" regime, weakly negative E_r is observed. In high T_i shots [14-15], experimental data shows small negative E_r , which corresponds to "Ion root" predicted by the neoclassical theory. Cases B~E in Fig.4 correspond to discharges in the Ion root or the Multiple root regime. The theoretical prediction for the dependence of the sign of E_r on the temperatures is consistent with experimental results in three magnetic field configurations, namely wide helical ripple parameters.

4. Summary

The radial potential profile was measured with HIBP in LHD. The potential at the plasma core was positive in the case of EC heating, namely high T_e , low n_e . In the low T_e case, the potential in the core was almost zero or negative. The radial electric field, E_r , was obtained from measured radial potential profile. Based on the condition of neoclassical ambipolarity, E_r is estimated theoretically and compared with experimental results. Theoretical predictions roughly coincide with the experimental results. The theoretical calculation of the sign of E_r (electron root and ion root) in the $T_i - T_e$ parameter space was also done, and compared with experimental results. The theoretical calculation based on neoclassical ambipolarity is consistent with the sign of E_r observed in experiments. Thus, we clarified that physics of neoclassical context is almost dominant in E_r formation, in wide plasma parameters of advanced high temperature plasmas. The results will provide a physical basis to consider further improved confinement scenarios utilizing E_r in helical plasmas.

Acknowledgements

The authors wish to thank the scientific and technical staff of LHD group for their continual support. This work was supported by MEXT Japan under Grants-in-Aid for Young Scientists (Nos. 18760640, 20686062), NIFS/NINS under the project of Formation of International Network for Scientific Collaborations, and NIFS09ULBB505, NIFS09ULBB515.

- [1] JOBES F. C., MARSHALL J. F., HICKOK R. L., "Plasma Density Measurement by Ion-Beam Probing", Phys. Rev. Lett. **22** (1969) 1042.
- [2] FUJISAWA A. et al., "A 6MeV Heavy Ion Beam Probe for the Large Helical Device", IEEE Trans. on Plasma Sci. **22** (1994) 395.
- [3] SHIMIZU A., IDO T., NISHIURA M. et al., "Present Status in the Development of 6 MeV Heavy Ion Beam Probe on LHD", J. Plasma Fusion Res. **2** (2007) S1098-1.
- [4] IDO T. et al., "Spatial Resolution of the Heavy Ion Beam Probe on LHD", J. Plasma Fusion Res. **2** (2007) S1100.
- [5] IDO T. et al., "6 MeV heavy ion beam probe on the Large Helical Device", Rev. Sci. Instrum. **77** (2006) 10F523.
- [6] SHIMIZU A., IDO T., NISHIURA M. et al., "Potential Measurement with the 6-MeV Heavy Ion Beam Probe of LHD", J. Plasma Fusion Res. **5** (2010) S1015.
- [7] SHIMIZU A., "Potential measurements with Heavy Ion Beam Probe system on LHD", Rev. Sci. Instrum. (2010) to be published.
- [8] IDO T. et al., "Development of 6-MeV Heavy Ion Beam Probe on LHD", Fusion Sci. Tech. **58** (2010) 436.
- [9] IDO T. et al., "Measurement of electrostatic potential fluctuation using heavy ion beam probe in large helical device", Rev. Sci. Instrum. **79** (2008) 10F318.
- [10] HAMADA Y., FUJISAWA A., IGUCHI H., NISHIZAWA A., KAWASUMI Y., "A tandem parallel plate analyzer", Rev. Sci. Instrum. **68** (1997) 2020.
- [11] FUJISAWA A., IGUCHI H. et al., "Active control of beam trajectories for heavy ion beam probe on helical magnetic configurations", Rev. Sci. Instrum. **63** (1992) 3694.
- [12] BEIDLER C. D., DHAESSELLER W. D., "A general solution of the ripple-averaged

- kinetic equation (GSRAKE)", Plasma Phys. Control. Fusion **37** (1995) 463.
- [13] YOKOYAMA M. et al., "Towards improved confinement: Analysis of the radial electric field in LHD", Nucl. Fusion **42** (2002) 143.
- [14] NAGAOKA K. et al., "Ion heating experiments and improvement of ion heat transport in LHD", Fusion Sci. Tech. **58** (2010) 46.
- [15] IDO T. et al., "Experimental study of radial electric field and electrostatic potential fluctuation in the Large Helical Device", 37th EPS conference on Plasma Physics, 21-25 June, 2010, Dublin, Ireland.
- [16] IDA K., SHIMOZUMA T., FUNABA H. et al., "Characteristics of Electron Heat Transport of Plasma with an Electron Internal-Transport Barrier in the Large Helical Device", Phys. Rev. Lett. **91** (2003) 085003.
- [17] SHIMOZUMA T., KUBO S. et al., "Transition phenomena and thermal transport properties in LHD plasmas with an electron internal transport barrier", Nucl. Fusion **45** (2005) 1396.